Journal of Computational Physics 242 (2013) 181–195

Contents lists available at SciVerse ScienceDirect

Journal of Computational Physics

journal homepage: www.elsevier.com/locate/jcp

# Arbitrary high-order $C^0$ tensor product Galerkin finite element methods for the electromagnetic scattering from a large cavity

Kui Du [a,*,1], Weiwei Sun [b,2], Xiaoping Zhang [c,3]

[a] School of Mathematical Sciences, Xiamen University, Xiamen 361005, China
[b] Department of Mathematics, City University of Hong Kong, Kowloon, Hong Kong
[c] School of Mathematics and Statistics, Wuhan University, Wuhan 430072, China

ARTICLE INFO

*Article history:*
Received 11 October 2012
Received in revised form 29 January 2013
Accepted 12 February 2013
Available online 24 February 2013

*Keywords:*
Helmholtz equation
Electromagnetic scattering
Tensor product FEM
Fast algorithm

ABSTRACT

The paper is concerned with the electromagnetic scattering from a large cavity embedded in an infinite ground plane. The electromagnetic cavity problem is described by the Helmholtz equation with a nonlocal boundary condition on the aperture of the cavity and Dirichlet (or Neumann) boundary conditions on the walls of the cavity. A tensor product Galerkin finite element method (FEM) is proposed, in which spaces of $C^0$ piecewise polynomials of degree $\kappa \geqslant 1$ are employed. By the fast Fourier transform and the Toeplitz-type structure of the approximation to the nonlocal operator in the nonlocal boundary condition, a fast algorithm is designed for solving the linear system arising from the cavity problem with (vertically) layered media, which requires $\mathcal{O}(N^2 \log N)$ operations on an $N \times N$ uniform partition. Numerical results for model problems illustrate the efficiency of the fast algorithm and exhibit the expected optimal global convergence rates of the finite element methods. Moreover, our numerical results also show that the high-order approximations are especially effective for problems with large wave numbers.



## 1. Introduction

Electromagnetic scattering is an important topic in modern computational electromagnetics due to its significant industrial and military applications, see, for example, [26] and the references therein. In many such applications, the accurate prediction of the radar cross section (RCS) of a cavity is necessary due to its dominance to the targets overall RCS. Examples of cavities include jet engine inlet ducts, exhaust nozzles, and cavity-backed antennas [4]. Mathematical analysis on existence and uniqueness of solutions of the cavity problem has been conducted recently in [3,6,33]. A variety of numerical methods including finite difference, finite element, boundary element methods, spectral methods, mode matching methods and hybrid methods have been developed for solving the cavity problem [7,8,10,15,24,27–29,31,36,39,41–43]. The computation is especially challenging when the cavities are large compared to the wavelength of the fields because of the highly oscillatory nature of the fields. A straightforward change of coordinates yields the equivalence of large wave number and large cavity problems. For convenience, without loss of generality, we focus primarily on large wave number problems in the discussion.

* Corresponding author. Tel.: +86 592 2580672.
*E-mail addresses:* kuidumath@yahoo.com (K. Du), maweiw@math.cityu.edu.hk (W. Sun), xpzhang.math@whu.edu.cn (X. Zhang).

[1] The research of this author was supported by the National Natural Science Foundation of China (Grant No. 11201392), the Natural Science Foundation of Fujian Province of China (No. 2012J05010) and the Doctoral Fund of Ministry of Education of China (No. 20120121120020).
[2] The work of this author was supported in part by a Grant from the Research Grants Council of the Hong Kong Special Administrative Region, China (Project No. CityU 9041546).
[3] The research of this author was supported by the National Natural Science Foundation of China (Grant No. 11101317).

0021-9991/$ - see front matter © 2013 Elsevier Inc. All rights reserved.
http://dx.doi.org/10.1016/j.jcp.2013.02.015

Mathematically, the two-dimensional electromagnetic cavity model (see Section 2) is described by the Helmholtz equation in the cavity with Dirichlet (or Neumann) boundary conditions on the walls of the cavity and a nonlocal boundary condition on the aperture of the cavity. For the Helmholtz problem with large wave numbers, due to the pollution effect [5,11,25] of the computed solution, low-order methods often require very fine meshes per wavelength, which leads to extremely large scale indefinite linear systems [18,37]. Furthermore, it is well known that error estimates strongly depend upon the wave number $k$. The error is proportional to $k^{\kappa+1}h^{\kappa}$, where $\kappa$ is the order of accuracy of the method and $h$ is the mesh size. So the number of points per wavelength needed for a given accuracy behaves like $k^{1/\kappa}$. Therefore, high order methods are more attractive for solving the Helmholtz problem with large wave numbers since they can offer relative higher accurate solutions by utilizing fewer mesh points. Many high-order methods have been proposed to solve different Helmholtz problems; see, for example, [12–14,22,23,30,32,42].

In this paper, we propose a tensor product finite element Galerkin (FEG) method with spaces of $C^0$ piecewise polynomials of degree $\kappa \geqslant 1$ employed for the numerical solution of the cavity problem. By the recently proposed matrix decomposition algorithms [21] and the Toeplitz-type structure (see Appendix A) of the discrete nonlocal operator in the nonlocal boundary condition, a fast algorithm for solving the linear systems arising from the cavity problem with (vertically) layered media is designed, which employs fast Fourier transforms and requires $\mathcal{O}(N^2 \log N)$ operations on an $N \times N$ uniform partition. Our fast algorithm can be viewed as a generalization of that given in [8] where a fast algorithm for solving low-order finite difference systems was proposed. We present numerical results for several examples which exhibit the expected optimal global convergence rates as well as efficiency of the fast algorithm. Numerical results for a model problem show that the FEG method with high-order approximations are especially effective for problems with large wave numbers.

A brief outline of the rest of this paper is as follows. In Section 2 the model scattering problem is formulated and further reduced to a bounded domain problem. We describe the tensor product finite element Galerkin method for the transverse magnetic case of the cavity problem in Section 3. The fast algorithm for solving the linear systems arising from the cavity problem with (vertically) layered media is introduced in Section 4. Issues on implementation and complexity of the algorithm are addressed. Section 5 is devoted to numerical experiments of the algorithm. Finally, Section 6 contains conclusions and a discussion of future work.

## 2. The electromagnetic cavity problem

Consider a time-harmonic electromagnetic plane wave incident on a cavity embedded in an infinite ground plane. Assume that the ground plane and walls of the cavity are perfect electric conductors (PEC). Assume that the medium is nonmagnetic with a constant permeability $\mu = \mu_0$ everywhere and a constant permittivity $\varepsilon = \varepsilon_0$ for free space, no currents are present and the fields are source free. Assume that the permittivity of the medium in the cavity $\varepsilon(\mathbf{x})$ is bounded, $\mathrm{Re}(\varepsilon(\mathbf{x})) \geqslant \gamma > 0$ and $\mathrm{Im}(\varepsilon(\mathbf{x})) \geqslant 0$. The total electric and magnetic fields $E$ and $H$ satisfy the following time-harmonic Maxwell's equations (time dependence $e^{-\mathrm{i}\omega t}$):

$$\nabla \times E - \mathrm{i}\omega\mu H = 0,$$
$$\nabla \times H + \mathrm{i}\omega\varepsilon E = 0,$$

where $\mathrm{i} = \sqrt{-1}$ is the imaginary unit and $\omega$ is the angular frequency. On the surface of the perfect electric conductors, the following boundary condition is satisfied for the total electric field

$$\nu \times E = 0,$$

where $\nu$ is the unit outward normal.

For simplicity, assume that the medium and the cavity have no variation with respect to the $z$-axis. We further assume the cavity has a rectangular cross section $\Omega = (0, a) \times (0, b)$. Denote the aperture and the walls of the cavity by $\Gamma = [0, a] \times \{b\}$ and $S = \partial\Omega \setminus \Gamma$, respectively. Let $\mathbb{R}_b = (-\infty, +\infty) \times \{b\}$ and $\Gamma^C = \mathbb{R}_b \setminus \Gamma$. Denote the upper half-plane by $\mathrm{U}_b^+$. See Fig. 1. Two fundamental polarizations, the transverse electric (TE) and the transverse magnetic (TM), are often considered in the study of the propagation of the scattered waves from the cavity.

- TM polarization: the magnetic field is transverse to the $z$-axis so that $E$ and $H$ are of the form $E = (0, 0, E_z),\ H = (H_x, H_y, 0)$.
- TE polarization: the electric field is transverse to the $z$-axis so that $E$ and $H$ are of the form $E = (E_x, E_y, 0),\ H = (0, 0, H_z)$.

To simplify the notation, let $u(x, y) = E_z(x, y)$ and $v(x, y) = H_z(x, y)$, respectively. Let $\varepsilon_r = \varepsilon(\mathbf{x})/\varepsilon_0$ be the relative permittivity of the medium and $k_0 = \omega\sqrt{\varepsilon_0\mu_0}$ the free space wave number.

For the TM polarization, we have

$$u = 0, \quad \text{on } \Gamma^C \cup S \tag{2.1}$$

by $\nu = (\nu_x, \nu_y, 0)$ and $\nu \times E = 0$. The time-harmonic Maxwell's equations reduce to the Helmholtz equation together with the boundary condition (2.1) and the Sommerfeld's radiation condition imposed at infinity,

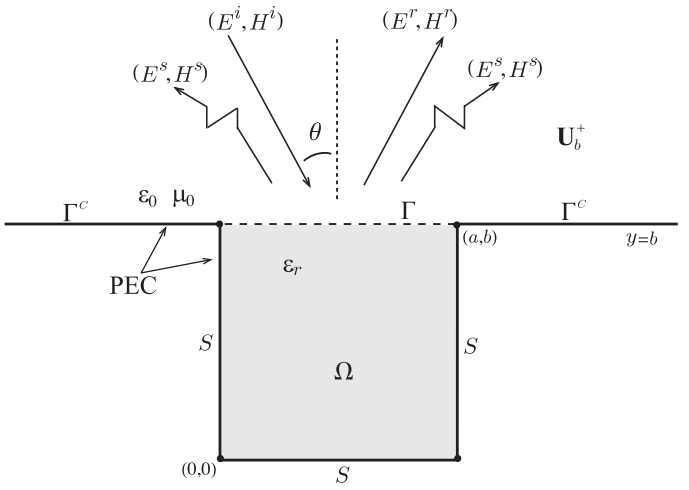


**Fig. 1.** Rectangular cavity geometry.

$$\begin{cases} \Delta u + k_0^2 \varepsilon_r u = f_{\mathrm{M}} & \text{in } \Omega \cup \mathrm{U}_b^+, \\ u = 0 & \text{on } \Gamma^C \cup S, \\ \lim\limits_{r\to\infty} \sqrt{r}(\partial_r u^s - \mathrm{i}k_0 u^s) = 0 & \text{at infinity}, \end{cases} \tag{2.2}$$

where $f_{\mathrm{M}}$ is the source term and $f_{\mathrm{M}} = 0$ in $\mathrm{U}_b^+$ and $u^s$ is the $z$-component of the scattered field.

For the TE polarization, we have

$$\partial_\nu v = 0, \quad \text{on } \Gamma^C \cup S \tag{2.3}$$

by $v = (v_x, v_y, 0), v \times E = 0$ and $\nabla \times H + \mathrm{i}\omega\varepsilon E = 0$. The time-harmonic Maxwell's equations reduce to the Helmholtz-type equation together with the boundary condition (2.3) and the Sommerfeld's radiation condition imposed at infinity,

$$\begin{cases} \nabla \cdot \left(\dfrac{1}{\varepsilon_r} \nabla v\right) + k_0^2 v = f_{\mathrm{E}} & \text{in } \Omega \cup \mathrm{U}_b^+, \\ \partial_\nu v = 0 & \text{on } \Gamma^C \cup S, \\ \lim\limits_{r\to\infty} \sqrt{r}(\partial_r v^s - \mathrm{i}k_0 v^s) = 0 & \text{at infinity}, \end{cases} \tag{2.4}$$

where $f_{\mathrm{E}}$ is the source term and $f_{\mathrm{E}} = 0$ in $\mathrm{U}_b^+$ and $v^s$ is the $z$-component of the scattered field.

The scattering problem in both cases is: For a given incident plane wave, determine the scattered fields in the cavity and the half space. Assume that a plane wave $u^i = e^{\mathrm{i}\alpha x - \mathrm{i}\beta(y-b)}$ is incident on the cavity from the above, where $\alpha = k_0 \sin\theta$, $\beta = k_0 \cos\theta$, and $-\pi/2 < \theta < \pi/2$ is the angle of incidence with respect to the positive $y$-axis. The $z$-components of the scattered fields can be expressed by

$$u^s = u - u^i + e^{\mathrm{i}\alpha x + \mathrm{i}\beta(y-b)}$$

and

$$v^s = v - u^i - e^{\mathrm{i}\alpha x + \mathrm{i}\beta(y-b)},$$

respectively.

If the fillings of the cavity do not protrude above the ground plane, we say the cavity is non-overfilled. Otherwise, it is overfilled. Since the medium in the upper half space is homogeneous for non-overfilled cavity problems, a so-called transparent (nonlocal) boundary condition can be obtained by using Green's function method [26] or the method of Fourier's transform [3]. We refer to [38,19] for the overfilled case. For the TM polarization, the scattering problem can be further reduced to a bounded domain problem:

$$\begin{cases} \Delta u + k_0^2 \varepsilon_r u = f_{\mathrm{M}} & \text{in } \Omega, \\ u = 0 & \text{on } S, \\ \partial_\nu u = \mathcal{T}_{\mathrm{M}}(u) + g_{\mathrm{M}} & \text{on } \Gamma, \end{cases} \tag{2.5}$$

where

$$\mathcal{T}_{\mathrm{M}}(u) = \frac{\mathrm{i}k_0}{2} \int_0^a \frac{1}{|x - x'|} H_1^{(1)}(k_0|x - x'|) u(x', b) \mathrm{d}x'$$

and

$$g_{\mathrm{M}}(x) = -2\mathrm{i}\beta e^{\mathrm{i}\alpha x}.$$

Here, $\not=$ denotes a Hadamard finite-part integral [40] and $H_\nu^{(1)}(z)$ is the Hankel function of the first kind [1]. For the TE polarization, the scattering problem can be further reduced to a bounded domain problem:

$$\begin{cases} \nabla\cdot\left(\dfrac{1}{\varepsilon_r}\nabla v\right) + k_0^2 v = f_{\mathrm{E}} & \text{in } \Omega, \\ \partial_\nu v = 0 & \text{on } S, \\ v = \mathcal{T}_{\mathrm{E}}(\partial_\nu v) + g_{\mathrm{E}} & \text{on } \Gamma, \end{cases} \tag{2.6}$$

where

$$\mathcal{T}_{\mathrm{E}}(\partial_\nu v) = -\frac{\mathrm{i}}{2}\int_0^a H_0^{(1)}(k_0|x-x\prime|)\frac{1}{\varepsilon_r}\frac{\partial v(x\prime,b)}{\partial \nu}\mathrm{d}x'$$

and

$$g_{\mathrm{E}}(x) = 2e^{\mathrm{i}\alpha x}.$$

In the next section, we propose a tensor product Galerkin finite element method for solving the TM case. A finite element method for the TE case can be designed analogously and will be reported elsewhere.

## 3. $\kappa$-order $C^0$ tensor product Galerkin finite element methods for the TM case

Define

$$H_{00}^{1/2}(\Gamma) := \left\{ w \in H^{1/2}(\Gamma) : \exists \widetilde{w} \in H^{1/2}(\mathbb{R}_b) \text{ such that } \widetilde{w} = 0 \text{ on } \Gamma^{\mathrm{C}} \text{ and } w = \widetilde{w}|_\Gamma \right\}.$$

Let

$$U := \{ w \in H^1(\Omega) : w = 0 \text{ on } S \text{ and } w|_\Gamma \in H_{00}^{1/2}(\Gamma) \}$$

equipped with the $H^1$-norm. The equivalent variational formulation of (2.5) is to find $u \in U$ such that

$$a^{\mathrm{M}}(u,w) = G^{\mathrm{M}}(w), \quad \text{for all } w \in U, \tag{3.1}$$

where

$$a^{\mathrm{M}}(u,w) = \int_\Omega (\nabla u\cdot\overline{\nabla w} - k_0^2\varepsilon_r u\overline{w})\mathrm{d}x\mathrm{d}y - \int_\Gamma \mathcal{T}_{\mathrm{M}}(u)\overline{w}\mathrm{d}x$$

and

$$G^{\mathrm{M}}(w) = \int_\Gamma g_{\mathrm{M}}\overline{w}\mathrm{d}x - \int_\Omega f_{\mathrm{M}}\overline{w}\mathrm{d}x\mathrm{d}y.$$

It was proved in [3,33] that the variational problem (3.1) has a unique solution $u \in U$.

We describe the $\kappa$-order $C^0$ tensor product Galerkin finite element methods for (3.1) as follows. For simplicity, let $\Omega = (0,1)\times(0,1)$. Let $\{L_j(t)\}_{j=0}^{\kappa}$ denote the basis of standard Lagrange interpolation to the $\kappa+1$ uniform mesh points $t_j = j/\kappa,\ j = 0,1,\ldots,\kappa$, on $[0,1]$. Then

$$L_j(t) = \frac{(t-t_0)(t-t_1)\cdots(t-t_{j-1})(t-t_{j+1})\cdots(t-t_\kappa)}{(t_j-t_0)(t_j-t_1)\cdots(t_j-t_{j-1})(t_j-t_{j+1})\cdots(t_j-t_\kappa)},$$

so that

$$L_j(t_i) = \delta_{ij} = \begin{cases} 0, & i \neq j, \\ 1, & i = j. \end{cases} \tag{3.2}$$

Let $\{x_i\}_{i=1}^N$ be a uniform mesh on $[0,1]$ such that $x_i = ih,\ i = 0,1,\ldots,N$, where $N$ is a positive integer and $h = 1/N$ is the mesh-size. For any integer $\kappa \geqslant 1$, let $\mathcal{S}_{\kappa,N}$ be the space of $C^0$ piecewise $\kappa$-order polynomials on $[0,1]$ defined by

$$\mathcal{S}_{\kappa,N} = \{ w \in C^0[0,1] : w|_{[x_{i-1},x_i]} \in P_\kappa,\ i = 1,\ldots,N \},$$

where $P_\kappa$ is the set of polynomials of degree $\leqslant \kappa$. We define a basis for $\mathcal{S}_{\kappa,N}$, $\{\psi_{i\kappa+j}(x)\}_{i,j=0}^{N-1,\kappa}$, by

$$\psi_0(x) = \begin{cases} L_0\left(\dfrac{x-x_0}{h}\right), & x_0 \leqslant x \leqslant x_1, \\ 0, & \text{otherwise}, \end{cases}$$

$$\psi_{i\kappa}(x)=\begin{cases} L_0\Big(\dfrac{x-x_i}{h}\Big), & x_i\leqslant x\leqslant x_{i+1},\\ L_\kappa\Big(\dfrac{x-x_{i-1}}{h}\Big), & x_{i-1}\leqslant x\leqslant x_i, \quad i=1,\ldots,N-1,\\ 0, & \text{otherwise},\end{cases}$$

$$\psi_{i\kappa+j}(x)=\begin{cases} L_j\Big(\dfrac{x-x_i}{h}\Big), & x_i\leqslant x\leqslant x_{i+1}, \quad i=0,\ldots,N-1,\ j=1,\ldots,\kappa-1,\\ 0, & \text{otherwise},\end{cases}$$

$$\psi_{\kappa N}(x)=\begin{cases} L_\kappa\Big(\dfrac{x-x_{N-1}}{h}\Big), & x_{N-1}\leqslant x\leqslant x_N,\\ 0, & \text{otherwise}.\end{cases}$$

Then, from (3.2),

$$\psi_i(jh/\kappa)=\delta_{ij},\quad i,j=0,1,\ldots,\kappa N.$$

Let

$$\mathcal{S}^{\mathcal{D}}_{\kappa,N}=\{w\in\mathcal{S}_{\kappa,N}: w(0)=w(1)=0\},\quad \mathcal{S}^{\mathcal{DN}}_{\kappa,M}=\{w\in\mathcal{S}_{\kappa,M}: w(0)=0\}.$$

In the $\kappa$-order $C^0$ tensor product Galerkin finite element method on an $N\times M$ partition of $\Omega$ for the variational problem (3.1), we seek $u^h\in\mathcal{S}^{\mathcal{D}}_{\kappa,N}\otimes\mathcal{S}^{\mathcal{DN}}_{\kappa,M}$, where $\otimes$ denotes the space tensor product, such that

$$a^{\mathrm{M}}(u^h,w^h)=G^{\mathrm{M}}(w^h),\quad \text{for all } w^h\in\mathcal{S}^{\mathcal{D}}_{\kappa,N}\otimes\mathcal{S}^{\mathcal{DN}}_{\kappa,M}. \tag{3.3}$$

If $\{\psi_n\}_{n=1}^{\kappa N-1}$ is a basis for $\mathcal{S}^{\mathcal{D}}_{\kappa,N}$, and $\{\phi_n\}_{n=1}^{\kappa M}$ is a basis for $\mathcal{S}^{\mathcal{DN}}_{\kappa,M}$, we may write

$$u^h(x,y)=\sum_{i=1}^{M_1}\sum_{j=1}^{M_2+1}u_{ij}\psi_i(x)\phi_j(y),\quad M_1=\kappa N-1,\quad M_2=\kappa M-1.$$

Then the Galerkin equation (3.3) with $w^h=\psi_m(x)\phi_n(y)$ become

$$\begin{aligned}&\sum_{i=1}^{M_1}\sum_{j=1}^{M_2+1}u_{ij}\left[(\psi_i',\psi_m')(\phi_j,\phi_n)+(\psi_i,\psi_m)(\phi_j',\phi_n')-k_0^2\int_\Omega\varepsilon_r(x,y)\psi_i(x)\psi_m(x)\phi_j(y)\phi_n(y)\mathrm{d}x\mathrm{d}y\right]-\sum_{i=1}^{M_1}u_{i,M_2+1}\\ &\quad\times\int_\Gamma\mathcal{T}_{\mathrm{M}}(\psi_i(x))\psi_m(x)\phi_n(1)\mathrm{d}x\\ &\quad=\int_\Gamma g_{\mathrm{M}}\psi_m(x)\phi_n(1)\mathrm{d}x-\int_\Omega f_{\mathrm{M}}\psi_m(x)\phi_n(y)\mathrm{d}x\mathrm{d}y,\end{aligned}$$

where

$$(\phi,\psi)=\int_0^1\phi(x)\psi(x)\mathrm{d}x.$$

Let

$$\begin{aligned}u_\Omega&=\left[u_{1,1},\ldots,u_{1,M_2},u_{2,1},\ldots,u_{2,M_2},\ldots,u_{M_1,1},\ldots,u_{M_1,M_2}\right]^{\mathrm{T}},\\ u_\Gamma&=\left[u_{1,M_2+1},u_{2,M_2+1},\ldots,u_{M_1,M_2+1}\right]^{\mathrm{T}}\end{aligned}$$

and

$$\begin{aligned}f_\Omega&=\left[f_{1,1},\ldots,f_{1,M_2},f_{2,1},\ldots,f_{2,M_2},\ldots,f_{M_1,1},\ldots,f_{M_1,M_2}\right]^{\mathrm{T}},\\ f_\Gamma&=\left[f_{1,M_2+1},f_{2,M_2+1},\ldots,f_{M_1,M_2+1}\right]^{\mathrm{T}},\end{aligned}$$

where

$$f_{i,j}=-\int_\Omega f_{\mathrm{M}}\psi_i(x)\phi_j(y)\mathrm{d}x\mathrm{d}y,\quad i=1,\ldots,M_1,\ j=1,\ldots,M_2$$

and

$$f_{i,M_2+1}=\int_0^1 g_{\mathrm{M}}\psi_i(x)\mathrm{d}x-\int_\Omega f_{\mathrm{M}}\psi_i(x)\phi_{M_2+1}(y)\mathrm{d}x\mathrm{d}y,\quad i=1,\ldots,M_1.$$

We obtain the linear system

$$\mathcal{A}\mathbf{u}:=\begin{bmatrix}A & B\\ B^{\mathrm{T}} & G\end{bmatrix}\begin{bmatrix}u_\Omega\\ u_\Gamma\end{bmatrix}=\begin{bmatrix}f_\Omega\\ f_\Gamma\end{bmatrix}=:\mathbf{f}, \tag{3.4}$$

where

$$A = A_1 \otimes B_2 + B_1 \otimes A_2 - k_0^2 E_0,$$
$$B = A_1 \otimes \mathbf{b}_2 + B_1 \otimes \mathbf{a}_2 - k_0^2 E_{M_2+1},$$
$$G = b^{(2)}_{M_2+1,M_2+1} A_1 + a^{(2)}_{M_2+1,M_2+1} B_1 - k_0^2 E_{M_2+1,M_2+1} - T,$$

with

$$A_1 = \left[a^{(1)}_{ij}\right]_{i,j=1}^{M_1}, \quad A_2 = \left[a^{(2)}_{ij}\right]_{i,j=1}^{M_2}, \quad B_1 = \left[b^{(1)}_{ij}\right]_{i,j=1}^{M_1}, \quad B_2 = \left[b^{(2)}_{ij}\right]_{i,j=1}^{M_2},$$
$$\mathbf{a}_2 = \left[a^{(2)}_{i,M_2+1}\right]_{i=1}^{M_2}, \quad \mathbf{b}_2 = \left[b^{(2)}_{i,M_2+1}\right]_{i=1}^{M_2},$$
$$a^{(1)}_{ij} = (\psi_i', \psi_j'), \quad a^{(2)}_{ij} = (\phi_i', \phi_j'), \quad b^{(1)}_{ij} = (\psi_i, \psi_j), \quad b^{(2)}_{ij} = (\phi_i, \phi_j),$$
$$T = [t_{ij}]_{i,j=1}^{M_1}, \quad t_{ij} = (\mathcal{T}_{\mathrm{M}}(\psi_i), \psi_j)$$

and

$$E_0 = [e_{ij}]_{i,j=1}^{M_1 M_2}, \quad e_{(i_1-1)M_2+i_2,(j_1-1)M_2+j_2} = \int_\Omega \varepsilon_r(x,y)\psi_{j_1}(x)\psi_{i_1}(x)\phi_{j_2}(y)\phi_{i_2}(y)\mathrm{d}x\mathrm{d}y,$$
$$E_{M_2+1} = \left[e^{(1)}_{ij}\right]_{i,j=1}^{M_1 M_2, M_1}, \quad e^{(1)}_{(i_1-1)M_2+i_2,j} = \int_\Omega \varepsilon_r(x,y)\psi_j(x)\psi_{i_1}(x)\phi_{M_2+1}(y)\phi_{i_2}(y)\mathrm{d}x\mathrm{d}y,$$
$$i_1, j_1 = 1, 2, \ldots, M_1, \quad i_2,\ j_2 = 1, 2, \ldots, M_2,$$
$$E_{M_2+1,M_2+1} = \left[e^{(2)}_{ij}\right]_{i,j=1}^{M_1}, \quad e^{(2)}_{ij} = \int_\Omega \varepsilon_r(x,y)\psi_j(x)\psi_i(x)\phi_{M_2+1}(y)\phi_{M_2+1}(y)\mathrm{d}x\mathrm{d}y.$$

By noting classical formulas [1]

$$\frac{H_1^{(1)}(z)}{z} = H_0^{(1)}(z) - \frac{\mathrm{d}H_1^{(1)}(z)}{\mathrm{d}z} = H_0^{(1)}(z) + \frac{\mathrm{d}^2 H_0^{(1)}(z)}{\mathrm{d}z^2}$$

and integration by parts, we have

$$t_{ij} = \frac{\mathrm{i}k_0}{2}\int_0^1\int_0^1 \frac{H_1^{(1)}(k_0|x-x'|)}{|x-x'|}\psi_i(x)\psi_j(x')\mathrm{d}x\mathrm{d}x' = \frac{\mathrm{i}}{2}\int_0^1\int_0^1 H_0^{(1)}(k_0|x-x'|)\left[k_0^2\psi_i(x)\psi_j(x') - \psi_i'(x)\psi_j'(x')\right]\mathrm{d}x\mathrm{d}x'.$$

Since $H_0^{(1)}(z)$ has a log-type singularity at $z = 0$, the above weakly singular integral can be evaluated easily [2].

Now we study the existence and uniqueness of the solution of the discrete system (3.4). The following lemma is essential.

**Lemma 3.1.** *The real and imaginary parts of the matrix T are symmetric negative definite and symmetric positive definite, respectively.*

**Proof.** By the following basic properties of Bessel functions [1]

$$H_0^{(1)}(z) = J_0(z) + \mathrm{i}Y_0(z),\ J_0(z) = \frac{2}{\pi}\int_0^1 \frac{\cos(zs)}{\sqrt{1-s^2}}\mathrm{d}s, \quad \text{and} \quad Y_0(z) = -\frac{2}{\pi}\int_1^\infty \frac{\cos(zs)}{\sqrt{s^2-1}}\mathrm{d}s,$$

we have

$$\begin{aligned}\mathrm{Re}(t_{ij}) &= -\frac{1}{2}\int_0^1\int_0^1 Y_0(k_0|x-x'|)\left[k_0^2\psi_i(x)\psi_j(x') - \psi_i'(x)\psi_j'(x')\right]\mathrm{d}x\mathrm{d}x' \\ &= \frac{1}{\pi}\int_0^1\int_0^1\int_1^\infty \frac{\cos(k_0(x-x')s)}{\sqrt{s^2-1}}\mathrm{d}s\left[k_0^2\psi_i(x)\psi_j(x') - \psi_i'(x)\psi_j'(x')\right]\mathrm{d}x\mathrm{d}x'\end{aligned}$$

and

$$\begin{aligned}\mathrm{Im}(t_{ij}) &= \frac{1}{2}\int_0^1\int_0^1 J_0(k_0|x-x'|)\left[k_0^2\psi_i(x)\psi_j(x') - \psi_i'(x)\psi_j'(x')\right]\mathrm{d}x\mathrm{d}x' \\ &= \frac{1}{\pi}\int_0^1\int_0^1\int_0^1 \frac{\cos(k_0(x-x')s)}{\sqrt{1-s^2}}\mathrm{d}s\left[k_0^2\psi_i(x)\psi_j(x') - \psi_i'(x)\psi_j'(x')\right]\mathrm{d}x\mathrm{d}x'.\end{aligned}$$

By integration by parts, we have

$$\mathrm{Re}(t_{ij}) = -\frac{k_0^2}{\pi}\int_1^\infty \sqrt{s^2-1}\int_0^1\int_0^1 \cos\left(k_0(x-x')s\right)\psi_i(x)\psi_j(x')\mathrm{d}x\mathrm{d}x'\mathrm{d}s$$
$$= -\frac{k_0^2}{2\pi}\int_1^\infty \sqrt{s^2-1}\int_0^1\int_0^1 \left[\mathrm{e}^{\mathrm{i}k_0(x-x')s}+\mathrm{e}^{\mathrm{i}k_0(x'-x)s}\right]\psi_i(x)\psi_j(x')\mathrm{d}x\mathrm{d}x'\mathrm{d}s$$

and

$$\mathrm{Im}(t_{ij}) = \frac{k_0^2}{\pi}\int_0^1 \sqrt{1-s^2}\int_0^1\int_0^1 \cos\left(k_0(x-x')s\right)\psi_i(x)\psi_j(x')\mathrm{d}x\mathrm{d}x'\mathrm{d}s$$
$$= \frac{k_0^2}{2\pi}\int_0^1 \sqrt{1-s^2}\int_0^1\int_0^1 \left[\mathrm{e}^{\mathrm{i}k_0(x-x')s}+\mathrm{e}^{\mathrm{i}k_0(x'-x)s}\right]\psi_i(x)\psi_j(x')\mathrm{d}x\mathrm{d}x'\mathrm{d}s.$$

For any vector $\mathbf{v} = [v_1, v_2, \ldots, v_{M_1}]$, we have

$$\sum_{i=1}^{M_1}\sum_{j=1}^{M_1}\int_0^1\int_0^1 \left[\mathrm{e}^{\mathrm{i}k_0(x-x')s}+\mathrm{e}^{\mathrm{i}k_0(x'-x)s}\right]\psi_i(x)v_i\psi_j(x')\overline{v}_j\mathrm{d}x\mathrm{d}x' = \sum_{i=1}^{M_1}\sum_{j=1}^{M_1}\int_0^1\int_0^1 \left[\mathrm{e}^{\mathrm{i}k_0xs}\psi_i(x)v_i\mathrm{e}^{-\mathrm{i}k_0x's}\psi_j(x')\overline{v}_j+\mathrm{e}^{-\mathrm{i}k_0xs}\psi_i(x)v_i\mathrm{e}^{\mathrm{i}k_0x's}\psi_j(x')\overline{v}_j\right]\mathrm{d}x\mathrm{d}x'$$
$$= \sum_{i=1}^{M_1}\int_0^1 \mathrm{e}^{\mathrm{i}k_0xs}\psi_i(x)v_i\mathrm{d}x\sum_{j=1}^{M_1}\int_0^1 \mathrm{e}^{-\mathrm{i}k_0xs}\psi_j(x)\overline{v}_j\mathrm{d}x$$
$$+\sum_{i=1}^{M_1}\int_0^1 \mathrm{e}^{-\mathrm{i}k_0xs}\psi_i(x)v_i\mathrm{d}x\sum_{j=1}^{M_1}\int_0^1 \mathrm{e}^{\mathrm{i}k_0xs}\psi_j(x)\overline{v}_j\mathrm{d}x = \left|\sum_{i=1}^{M_1}\int_0^1 \mathrm{e}^{\mathrm{i}k_0xs}\psi_i(x)v_i\mathrm{d}x\right|^2$$
$$+\left|\sum_{i=1}^{M_1}\int_0^1 \mathrm{e}^{-\mathrm{i}k_0xs}\psi_i(x)v_i\mathrm{d}x\right|^2.$$

For simplicity, let

$$\eta(s) = \left|\sum_{i=1}^{M_1}\int_0^1 \mathrm{e}^{\mathrm{i}k_0xs}\psi_i(x)v_i\mathrm{d}x\right|^2 + \left|\sum_{i=1}^{M_1}\int_0^1 \mathrm{e}^{-\mathrm{i}k_0xs}\psi_i(x)v_i\mathrm{d}x\right|^2.$$

Then we obtain

$$\mathbf{v}(\mathrm{Re}(T))\mathbf{v}^{\mathrm{H}} = -\frac{k_0^2}{2\pi}\int_1^\infty \sqrt{s^2-1}\eta(s)\mathrm{d}s$$

and

$$\mathbf{v}(\mathrm{Im}(T))\mathbf{v}^{\mathrm{H}} = \frac{k_0^2}{2\pi}\int_0^1 \sqrt{1-s^2}\eta(s)\mathrm{d}s.$$

Therefore, $\mathrm{Re}(T)$ is symmetric negative definite and $\mathrm{Im}(T)$ is symmetric positive definite. □

To show the uniqueness of the solution to the system (3.4), it suffices to prove that the system (3.4) has only the zero solution when $f_{\mathrm{M}} = 0$ and $g_{\mathrm{M}} = 0$. Since $\mathrm{Im}(\varepsilon_r) \geqslant 0$, we have $\mathrm{Im}(a^{\mathrm{M}}(u^h, u^h)) \geqslant u_\Gamma^{\mathrm{H}}\mathrm{Im}(T)u_\Gamma$. It follows from $u_\Gamma^{\mathrm{H}}\mathrm{Im}(T)u_\Gamma = 0$ and Lemma 3.1 that $u_\Gamma = 0$. By utilizing the approach in [8, Theorem 4.1], we can further deduce that $u_\Omega = 0$. Then we have the following theorem.

**Theorem 3.2.** *The linear system (3.4) attains a unique solution.*

In the rest of this section, we specify the structures of the matrices in (3.4). These structures are important in designing the fast algorithm given in Section 4. The matrices $A_1, A_2, B_1$ and $B_2$ are band matrices with bandwidth $2\kappa+1$ and can be obtained easily from the corresponding one-dimensional stiffness and mass matrices, whose sparsity structure is shown in Fig. 2, where the shaded overlapping square blocks are $(\kappa+1)\times(\kappa+1)$ matrices. It is obvious that, for $\kappa = 1$, the matrix $T$ is a symmetric Toeplitz matrix. For larger $\kappa$, the next theorem shows that the matrix $T$ has a Toeplitz-type structure. For a proof of this theorem, see the appendix.

**Theorem 3.3.** *The matrix $T = [t_{ij}]_{i,j=1}^{\kappa N-1}$ is bisymmetric, i.e.,*

$$t_{ij} = t_{ji}, \quad t_{ij} = t_{\kappa N-i,\kappa N-j} \quad \text{for } i,j = 1,2,\ldots,\kappa N-1.$$

*Moreover, it can be reordered to become a symmetric $\kappa\times\kappa$ block matrix with Toeplitz blocks.*

## 4. A fast algorithm

In this section we propose a fast algorithm for solving the rectangular cavity problem with vertically layered media inside. For this case, we have $\varepsilon_r = \varepsilon_r(y)$. Let $e_{ij}^y = (\varepsilon_r\phi_i, \phi_j)$. Then the matrices $E_0$, $E_{M_2+1}$ and $E_{M_2+1,M_2+1}$ in the linear system (3.4) are, respectively,

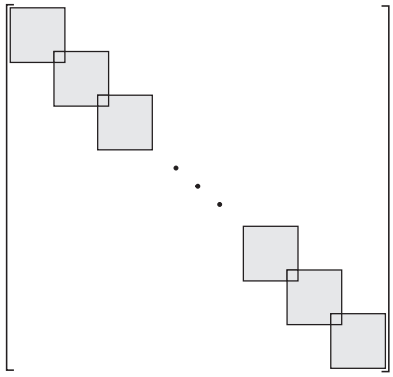

**Fig. 2.** The sparsity structure of the one-dimensional stiffness and mass matrices.

$$E_0 = B_1 \otimes E^y, \quad E^y = \left[e^y_{ij}\right]_{i,j=1}^{M_2},$$
$$E_{M_2+1} = B_1 \otimes \mathbf{e}^y, \quad \mathbf{e}^y = \left[e^y_{i,M_2+1}\right]_{i=1}^{M_2},$$
$$E_{M_2+1,M_2+1} = e^y_{M_2+1,M_2+1} B_1.$$

Therefore, the global finite element matrix $\mathcal{A}$ can be rewritten as

$$\mathcal{A} = \begin{bmatrix} A_1 \otimes B_2 + B_1 \otimes C_2 & A_1 \otimes \mathbf{b}_2 + B_1 \otimes \mathbf{c}_2 \\ A_1 \otimes \mathbf{b}_2^{\mathrm{T}} + B_1 \otimes \mathbf{c}_2^{\mathrm{T}} & cA_1 + dB_1 - T \end{bmatrix}$$

with

$$C_2 = A_2 - k_0^2 E^y, \quad \mathbf{c_2} = \mathbf{a}_2 - k_0^2 \mathbf{e}^y, \quad c = b^{(2)}_{M_2+1,M_2+1}, \quad d = a^{(2)}_{M_2+1,M_2+1} - k_0^2 e^y_{M_2+1,M_2+1}.$$

We note that the matrix $C_2$ has the same sparsity structure as that of the matrix $B_2$, and the vector $\mathbf{c_2}$ has the same sparsity structure as that of the vector $\mathbf{b_2}$.

Next, we propose a fast algorithm for solving the linear system (3.4). For the matrices $A_1$ and $B_1$, there exist a block diagonal matrix $Z$ and a permutation matrix $P$ (see [21] for more details) such that

$$Z^{\mathrm{T}} P S_{\kappa N-1} A_1 S_{\kappa N-1} P^{\mathrm{T}} Z = \Lambda =: \mathrm{diag}\{\lambda_1, \lambda_2, \ldots, \lambda_{\kappa N-1}\}$$

and

$$P S_{\kappa N-1} B_1 S_{\kappa N-1} P^{\mathrm{T}} = I,$$

where $S_\ell$ denotes the discrete Fourier–sine transformation

$$S_\ell = \left[\sqrt{\frac{2}{\ell+1}}\left(\sin\frac{ij\pi}{\ell+1}\right)\right]_{i,j=1}^{\ell},$$

$I$ denotes the identity matrix whose dimension is clear from the context, and

$$Z = \mathrm{diag}\{Z_1, \ldots, Z_{N-1}, Z_N, Z_{N+1}\},$$

$Z_i, i = 1, 2, \ldots N-1$ are matrices of order $\kappa, Z_N$ is a matrix of order $(\kappa-1)/2$ (if $\kappa$ is odd) or $\kappa/2$ (if $\kappa$ is even), $Z_{N+1}$ is a matrix of order $(\kappa-1)/2$ (if $\kappa$ is odd) or $\kappa/2-1$ (if $\kappa$ is even). In the rest of this section, let

$$\tilde{u}_\Omega = \left[(Z^{-1} P S_{\kappa N-1}) \otimes I\right] u_\Omega, \quad \tilde{u}_\Gamma = Z^{-1} P S_{\kappa N-1} u_\Gamma,$$

and

$$\tilde{f}_\Omega = \left[(Z^{\mathrm{T}} P S_{\kappa N-1}) \otimes I\right] f_\Omega, \quad \tilde{f}_\Gamma = Z^{\mathrm{T}} P S_{\kappa N-1} f_\Gamma.$$

Multiplying both side of (3.4) by

$$\begin{bmatrix} (Z^{\mathrm{T}} P S_{\kappa N-1}) \otimes I & \\ & Z^{\mathrm{T}} P S_{\kappa N-1} \end{bmatrix}$$

yields

$$\begin{bmatrix} \Lambda\otimes B_2 + I\otimes C_2 & \Lambda\otimes \mathbf{b}_2 + I\otimes \mathbf{c}_2 \\ \Lambda\otimes \mathbf{b}_2^{\mathrm{T}} + I\otimes \mathbf{c}_2^{\mathrm{T}} & c\Lambda + dI - \widetilde{T} \end{bmatrix} \begin{bmatrix} \tilde{u}_\Omega \\ \tilde{u}_\Gamma \end{bmatrix} = \begin{bmatrix} \tilde{f}_\Omega \\ \tilde{f}_\Gamma \end{bmatrix}, \tag{4.1}$$

where $\widetilde{T} = Z^{\mathrm{T}} P S_{\kappa N-1} T S_{\kappa N-1} P^{\mathrm{T}} Z$. By the first system of (4.1), we have $\kappa N - 1$ linear systems

$$Q_i \mathbf{x}_i + \tilde{u}_i^\Gamma \mathbf{y}_i = \mathbf{z}_i, \quad i = 1, 2, \ldots, \kappa N - 1, \tag{4.2}$$

where $Q_i = \lambda_i B_2 + C_2$ is a symmetric band matrix with bandwidth $2\kappa + 1$, $\mathbf{y}_i = \lambda_i \mathbf{b}_2 + \mathbf{c}_2$ is a vector with nonzero elements located in the last $\kappa$ positions, $\mathbf{x}_i$ and $\mathbf{z}_i$ are $(\kappa M - 1)$-vectors and $\tilde{u}_i^\Gamma$ are scalars such that

$$\begin{bmatrix} \mathbf{x}_1 \\ \mathbf{x}_2 \\ \vdots \\ \mathbf{x}_{\kappa N-1} \end{bmatrix} = \tilde{u}_\Omega, \quad \begin{bmatrix} \tilde{u}_1^\Gamma \\ \tilde{u}_2^\Gamma \\ \vdots \\ \tilde{u}_{\kappa N-1}^\Gamma \end{bmatrix} = \tilde{u}_\Gamma, \quad \begin{bmatrix} \mathbf{z}_1 \\ \mathbf{z}_2 \\ \vdots \\ \mathbf{z}_{\kappa N-1} \end{bmatrix} = \tilde{f}_\Omega.$$

Let $Q_i = L_i U_i$ be the LU factorization with partial pivoting, where $U_i$ is a upper triangular matrix and $L_i$ is a product of lower triangular and permutation matrices. We have $\widehat{U}_i \hat{\mathbf{x}}_i + \tilde{u}_i^\Gamma \widehat{L}_i \hat{\mathbf{y}}_i = \hat{\mathbf{z}}_i$. Here, $\widehat{U}_i$ and $\widehat{L}_i$ are the lower-right $\kappa \times \kappa$ principal submatrices of $U_i$ and $L_i^{-1}$ respectively; and $\hat{\mathbf{x}}_i$, $\hat{\mathbf{y}}_i$ and $\hat{\mathbf{z}}_i$ are the vectors consisting of the last $\kappa$ elements of $\mathbf{x}_i$, $\mathbf{y}_i$ and $L_i^{-1}\mathbf{z}_i$, respectively. If $\widehat{U}_i$ is nonsingular, we have

$$\hat{\mathbf{x}}_i = \widehat{U}_i^{-1} \hat{\mathbf{z}}_i - \tilde{u}_i^\Gamma D_i \hat{\mathbf{y}}_i, \quad \text{with } D_i = \widehat{U}_i^{-1} \widehat{L}_i. \tag{4.3}$$

Substituting (4.3) into the second system of (4.1) yields

$$(c\Lambda + dI - D - \widetilde{T})\tilde{u}_\Gamma = \tilde{f}_\Gamma - \mathbf{g}, \tag{4.4}$$

where

$$\mathbf{g} = [g_1,\ g_2,\ \ldots, g_{\kappa N-1}]^{\mathrm{T}} \quad \text{and} \quad D = \mathrm{diag}\{d_1, d_2, \ldots, d_{\kappa N-1}\}$$

with

$$g_i = \hat{\mathbf{y}}_i^{\mathrm{T}} \widehat{U}_i^{-1} \hat{\mathbf{z}}_i \quad \text{and} \quad d_i = \hat{\mathbf{y}}_i^{\mathrm{T}} D_i \hat{\mathbf{y}}_i.$$

Solving the linear system (4.4) gives the solution $\tilde{u}_\Gamma$ on the interface $\Gamma$. The rest of the unknowns can be obtained by solving the systems (4.2). If the matrix $\widehat{U}_i$ is singular (or nearly singular) for some index $i \in \mathcal{J}_s$, where $\mathcal{J}_s$ is a subset of the set $\{1, 2, \ldots, \kappa N - 1\}$, a special treatment can be used, see [8, Section 3] for details. In all of our numerical tests, $\mathcal{J}_s$ is empty, i.e., it suffices to solve the system (4.4). We obtain the following fast algorithm.

**Algorithm I.** The fast algorithm for electromagnetic cavity problems

| | |
|---|---|
| (i) | Generate the matrix $T$. |
| (ii) | Generate the matrix $Z$ and $\Lambda$. |
| (iii) | Calculate $\tilde{f}_\Omega = [(Z^{\mathrm{T}} P S_{\kappa N-1}) \otimes I] f_\Omega$ and $\tilde{f}_\Gamma = Z^{\mathrm{T}} P S_{\kappa N-1} f_\Gamma$. |
| (iv) | Calculate the LU factorization with partial pivoting to get $D$ and $\mathbf{g}$. |
| (v) | Solve the interface system (4.4) for $\tilde{u}_\Gamma$. |
| (vi) | Solve the linear systems (4.2) for $\tilde{u}_\Omega$. |
| (vii) | Calculate $u_\Omega = [(S_{\kappa N-1} P^{\mathrm{T}} Z) \otimes I]\tilde{u}_\Omega$ and $u_\Gamma = S_{\kappa N-1} P^{\mathrm{T}} Z \tilde{u}_\Gamma$. |

We analyze the computational cost of Algorithm I below. By the special structure of the matrix $T$ (see the appendix), it requires $\mathcal{O}(\kappa^4 N)$ function evaluations to generate $T$. In step (ii), one needs to solve $N + 1$ small generalized eigenvalue problems and the cost is $\mathcal{O}(\kappa^3 N)$. In step (iii), one needs to calculate the matrix vector products involving the matrices $S_{\kappa N-1}$ and $Z$. By a standard FFT-sine code, the cost for calculating the product of the matrix $S_{\kappa N-1}$ and a vector is $\mathcal{O}(\kappa N \log(\kappa N))$. By the block diagonal structure of $Z$, the cost for calculating the product of the matrix $Z$ and a vector is $\mathcal{O}(\kappa^2 N)$. Therefore, the cost of step (iii) is $\mathcal{O}(\kappa^2 MN \log(\kappa N)) + \mathcal{O}(\kappa^3 MN)$. In step (iv), one needs to calculate $\kappa N - 1$ LU factorizations. By the banded structure, the cost of one LU factorization is $\mathcal{O}(\kappa^3 M)$. Therefore, the cost of step (iv) is $\mathcal{O}(\kappa^4 MN)$. In step (v), we use a preconditioned Krylov subspace method [34] to solve the interface system (4.4). Since $T$ can be reordered to become a block matrix with Toeplitz block, the cost of each iteration is $\mathcal{O}(\kappa N \log(\kappa N)) + \mathcal{O}(\kappa^2 N)$. The cost of step (vi) is $\mathcal{O}(\kappa^4 MN)$. The cost of step (vii) is $\mathcal{O}(\kappa^2 MN \log(\kappa N)) + \mathcal{O}(\kappa^3 MN)$. The computational cost for each step of Algorithm I is summarized in Table 1.

In this paper, for the interface system (4.4), we use the diagonal matrix

$$c\Lambda + (d - \mathrm{i}k_0)I - D \tag{4.5}$$

as a preconditioner, which is the coefficient matrix of the corresponding interface system from the following physically approximate model:

**Table 1**
Computational cost of Algorithm I for an $N \times M$ partition of $\Omega$ ($q$ is the number of iterations of the Krylov subspace method).

| Step | Computational cost |
|---|---|
| (i) | $\mathcal{O}(\kappa^4 N)$ |
| (ii) | $\mathcal{O}(\kappa^3 N)$ |
| (iii) | $\mathcal{O}(\kappa^2 MN \log(\kappa N)) + \mathcal{O}(\kappa^3 MN)$ |
| (iv) | $\mathcal{O}(\kappa^4 MN)$ |
| (v) | $\mathcal{O}(q\kappa N \log(\kappa N)) + \mathcal{O}(q\kappa^2 N)$ |
| (vi) | $\mathcal{O}(\kappa^4 MN)$ |
| (vii) | $\mathcal{O}(\kappa^2 MN \log(\kappa N)) + \mathcal{O}(\kappa^3 MN)$ |

$$\begin{cases} \Delta u + k_0^2 \varepsilon_r u = f_{\mathrm{M}} & \text{in } \Omega, \\ u = 0 & \text{on } S, \\ \partial_n u = \mathrm{i} k_0 u + g_{\mathrm{M}} & \text{on } \Gamma. \end{cases}$$

This preconditioner has been tested for a finite difference discretization of (2.5) in [28]. Numerical experiments show that the number of iterations is independent of the mesh size and grows linearly with respect to the wave number $k_0$. See the numerical results in Section 5. The optimal sine transform based preconditioning technique for the finite difference discretization of cavity problems has been considered in [20]. The reported number of iterations is independent of the mesh size and the wave number. For $\kappa = 1$, since the matrix $T$ in (3.4) has symmetric Toeplitz structure, the optimal sine transform based preconditioner can be obtained in $\mathcal{O}(N)$ operations [16]. For larger $\kappa$, how to construct the optimal sine transform based preconditioner is being considered.

## 5. Numerical results

In this section, we report numerical results to illustrate the accuracy and efficiency of our algorithm. All computations are performed with MATLAB R2012a.

*Example 1*

Consider an artificial example defined by (2.5) with $\Omega = (0,1) \times (0,1)$ to test the accuracy of our methods. The functions $f_{\mathrm{M}}(x,y)$ and $g_{\mathrm{M}}(x)$ are chosen such that the exact solution is

$$u(x,y) = \mathrm{e}^{xy} \sin(k_0 x) \sin\left(\left(k_0 + \frac{\pi}{2}\right) y\right).$$

In Tables 2 and 3, we present errors and the corresponding convergence rates when $\kappa = 1,2,3,4,5$ in the $L^2$ and $H^1$ norms, for $k_0 = 4\pi, 8\pi, 16\pi, 32\pi$, respectively. Convergence rates in the various norms are determined using the formula

$$\mathrm{Rate} = \frac{\log(e_{N/2}/e_N)}{\log 2},$$

where $e_N$ is the error corresponding to the $N \times N$ partition of $\Omega$. As expected, the convergence rates for the $L^2$ and $H^1$ norms are $\kappa + 1$ and $\kappa$, respectively. We observe that lower-order approximations require much more mesh points to obtain a reasonable accuracy for large wave number problems, compared with high-order approximations.

Next, we report computational results for two cavity problems, a problem with a layered heterogeneous medium (Example 2) and a standard test problem with a homogeneous medium (Example 3), to test our algorithm. All the cases considered here are source free. Our focus is on the efficiency of our algorithm to solve the discrete linear systems. Because the coefficient matrix in the interface system (4.4) and the preconditioner (4.5) are both complex symmetric, the preconditioned conjugate orthogonal conjugate gradient method (COCG) [35] is used. The iteration is terminated at the $q$-th iteration if the residual satisfies $\|r_q\|_2 / \|f_\Gamma - \mathbf{g}\|_2 \leqslant 10^{-5}$.

The physical parameter of interest is the RCS, which is defined by

$$\sigma(\varphi) = \frac{4}{k_0} |P(\varphi)|^2$$

where $\varphi$ is the observation angle with respect to the positive $y$-axis and $P(\varphi)$ is the far-field coefficient given by

$$P(\varphi) = \frac{k_0}{2} \sin\varphi \int_0^a u \mathrm{e}^{\mathrm{i} k_0 x \cos\varphi} \mathrm{d}x.$$

When the incident and observation directions are the same, we have the backscatter RCS

**Table 2**
Errors and convergence rates in the $L^2$ and $H^1$ norms: Example 1 with $k_0 = 4\pi, 8\pi$.

| $\kappa$ | $N$ | $k_0 = 4\pi$ | | | | $k_0 = 8\pi$ | | | |
|---|---|---|---|---|---|---|---|---|---|
| | | $L^2$ Error | Rate | $H^1$ Error | Rate | $L^2$ Error | Rate | $H^1$ Error | Rate |
| 1 | 16 | 6.736e−02 | – | 3.139e+00 | – | 2.184e−01 | – | 1.177e+01 | – |
| | 32 | 1.776e−02 | 1.923 | 1.564e+00 | 1.006 | 6.556e−02 | 1.736 | 5.885e+00 | 1.001 |
| | 64 | 4.504e−03 | 1.980 | 7.806e−01 | 1.002 | 1.729e−02 | 1.923 | 2.925e+00 | 1.008 |
| 2 | 16 | 2.789e−03 | – | 3.423e−01 | – | 2.028e−02 | – | 2.422e+00 | – |
| | 32 | 3.470e−04 | 3.007 | 8.578e−02 | 1.997 | 2.499e−03 | 3.021 | 6.116e−01 | 1.986 |
| | 64 | 4.331e−05 | 3.002 | 2.146e−02 | 1.999 | 3.102e−04 | 3.010 | 1.532e−01 | 1.997 |
| 3 | 16 | 1.330e−04 | – | 2.437e−02 | – | 1.825e−03 | – | 3.307e−01 | – |
| | 32 | 8.382e−06 | 3.988 | 3.061e−03 | 2.993 | 1.168e−04 | 3.965 | 4.196e−02 | 2.978 |
| | 64 | 5.251e−07 | 3.997 | 3.831e−04 | 2.998 | 7.350e−06 | 3.991 | 5.264e−03 | 2.995 |
| 4 | 16 | 5.272e−06 | – | 1.340e−03 | – | 1.355e−04 | – | 3.418e−02 | – |
| | 32 | 1.653e−07 | 4.995 | 8.399e−05 | 3.996 | 4.269e−06 | 4.988 | 2.165e−03 | 3.981 |
| | 64 | 5.170e−09 | 4.999 | 5.253e−06 | 3.999 | 1.337e−07 | 4.997 | 1.358e−04 | 3.995 |
| 5 | 16 | 1.816e−07 | – | 5.669e−05 | – | 8.999e−06 | – | 2.791e−03 | – |
| | 32 | 2.862e−09 | 5.988 | 1.781e−06 | 4.992 | 1.449e−07 | 5.956 | 8.856e−05 | 4.978 |
| | 64 | 4.480e−11 | 5.997 | 5.574e−08 | 4.998 | 2.283e−09 | 5.988 | 2.778e−06 | 4.995 |

**Table 3**
Errors and convergence rates in the $L^2$ and $H^1$ norms: Example 1 with $k_0 = 16\pi,\ 32\pi$.

| $\kappa$ | $N$ | $k_0 = 16\pi$ | | | | $k_0 = 32\pi$ | | | |
|---|---|---|---|---|---|---|---|---|---|
| | | $L^2$ Error | Rate | $H^1$ Error | Rate | $L^2$ Error | Rate | $H^1$ Error | Rate |
| 1 | 64 | 6.504e−02 | – | 1.141e+01 | – | 2.151e−01 | – | 4.512e+01 | – |
| | 128 | 1.716e−02 | 1.922 | 5.664e+00 | 1.010 | 6.491e−02 | 1.729 | 2.248e+01 | 1.005 |
| | 256 | 4.351e−03 | 1.980 | 2.825e+00 | 1.004 | 1.713e−02 | 1.922 | 1.115e+01 | 1.011 |
| 2 | 64 | 2.378e−03 | – | 1.161e+00 | – | 1.900e−02 | – | 8.980e+00 | – |
| | 128 | 2.946e−04 | 3.013 | 2.909e−01 | 1.997 | 2.322e−03 | 3.032 | 2.265e+00 | 1.987 |
| | 256 | 3.673e−05 | 3.004 | 7.276e−02 | 1.999 | 2.875e−04 | 3.014 | 5.675e−01 | 1.997 |
| 3 | 64 | 1.105e−04 | – | 7.825e−02 | – | 1.669e−03 | – | 1.196e+00 | – |
| | 128 | 6.944e−06 | 3.992 | 9.813e−03 | 2.995 | 1.077e−04 | 3.954 | 1.514e−01 | 2.981 |
| | 256 | 4.347e−07 | 3.998 | 1.228e−03 | 2.999 | 6.768e−06 | 3.992 | 1.898e−02 | 2.996 |
| 4 | 64 | 3.894e−06 | – | 3.941e−03 | – | 1.193e−04 | – | 1.192e−01 | – |
| | 128 | 1.218e−07 | 4.999 | 2.472e−04 | 3.995 | 3.733e−06 | 4.998 | 7.550e−03 | 3.981 |
| | 256 | 3.806e−09 | 5.000 | 1.546e−05 | 3.999 | 1.167e−07 | 5.000 | 4.735e−04 | 3.995 |
| 5 | 64 | 1.316e−07 | – | 1.583e−04 | – | 7.814e−06 | – | 9.497e−03 | – |
| | 128 | 2.075e−09 | 5.987 | 4.963e−06 | 4.995 | 1.262e−07 | 5.952 | 3.006e−04 | 4.982 |
| | 256 | 3.277e−11 | 5.985 | 1.552e−07 | 4.999 | 1.990e−09 | 5.987 | 9.422e−06 | 4.995 |

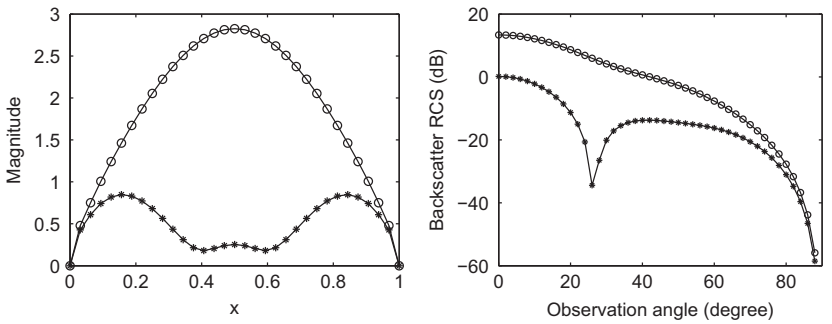


**Fig. 3.** Aperture electric field (left) and backscatter RCS (right) at normal incidence ($\theta = 0$) for Example 3 with $k_0 = 2\pi$. The line with marker ∘∘∘ indicates the result for $\varepsilon_r = 1$ and the line with marker ∗∗∗ indicates the result for $\varepsilon_r = 4 + \mathrm{i}$.

$$\text{Backscatter RCS}(\varphi) = 10\log_{10}\sigma(\varphi)\ \text{dB}.$$

*Example 2*

Consider the cavity $\Omega = (0,1) \times (0,1)$ filled with the following layered heterogeneous medium with relative permittivity $\varepsilon_r$:

**Table 4**
Number of iterations of the preconditioned COCG solver for the interface system (4.4): Example 2 with $\varepsilon_r$ in (5.1).

| $k_0$ | $2\pi$ | | | $4\pi$ | | | $8\pi$ | | | $16\pi$ | | | $32\pi$ | | |
|---|---|---|---|---|---|---|---|---|---|---|---|---|---|---|---|
| $N$ | 16 | 32 | 64 | 32 | 64 | 128 | 64 | 128 | 256 | 128 | 256 | 512 | 192 | 256 | 512 |
| $\kappa = 1$ | 6 | 7 | 8 | 9 | 10 | 11 | 14 | 15 | 15 | 19 | 19 | 22 | 28 | 29 | 34 |
| $\kappa = 2$ | 7 | 8 | 8 | 10 | 10 | 11 | 14 | 15 | 15 | 19 | 20 | 21 | 32 | 32 | 34 |
| $\kappa = 3$ | 8 | 8 | 8 | 10 | 10 | 11 | 15 | 15 | 16 | 20 | 20 | 21 | 32 | 33 | 34 |
| $\kappa = 4$ | 8 | 8 | 8 | 10 | 11 | 11 | 15 | 16 | 16 | 20 | 21 | 21 | 31 | 34 | 35 |
| $\kappa = 5$ | 8 | 8 | 8 | 10 | 11 | 11 | 15 | 16 | 16 | 20 | 21 | 21 | 33 | 34 | 35 |

**Table 5**
Number of iterations of the preconditioned COCG solver for the interface system (4.4): Example 3 with $\varepsilon_r = 1$.

| $k_0$ | $2\pi$ | | | $4\pi$ | | | $8\pi$ | | | $16\pi$ | | | $32\pi$ | | |
|---|---|---|---|---|---|---|---|---|---|---|---|---|---|---|---|
| $N$ | 16 | 32 | 64 | 32 | 64 | 128 | 64 | 128 | 256 | 128 | 256 | 512 | 192 | 256 | 512 |
| $\kappa = 1$ | 6 | 7 | 7 | 9 | 10 | 10 | 13 | 14 | 15 | 20 | 21 | 22 | 28 | 29 | 31 |
| $\kappa = 2$ | 7 | 8 | 8 | 10 | 10 | 10 | 14 | 15 | 15 | 21 | 22 | 23 | 27 | 29 | 30 |
| $\kappa = 3$ | 8 | 8 | 8 | 10 | 10 | 11 | 14 | 16 | 15 | 22 | 22 | 23 | 28 | 29 | 30 |
| $\kappa = 4$ | 7 | 8 | 8 | 10 | 11 | 11 | 15 | 15 | 16 | 22 | 23 | 23 | 29 | 30 | 30 |
| $\kappa = 5$ | 8 | 8 | 8 | 10 | 11 | 11 | 15 | 15 | 16 | 22 | 23 | 23 | 29 | 30 | 31 |

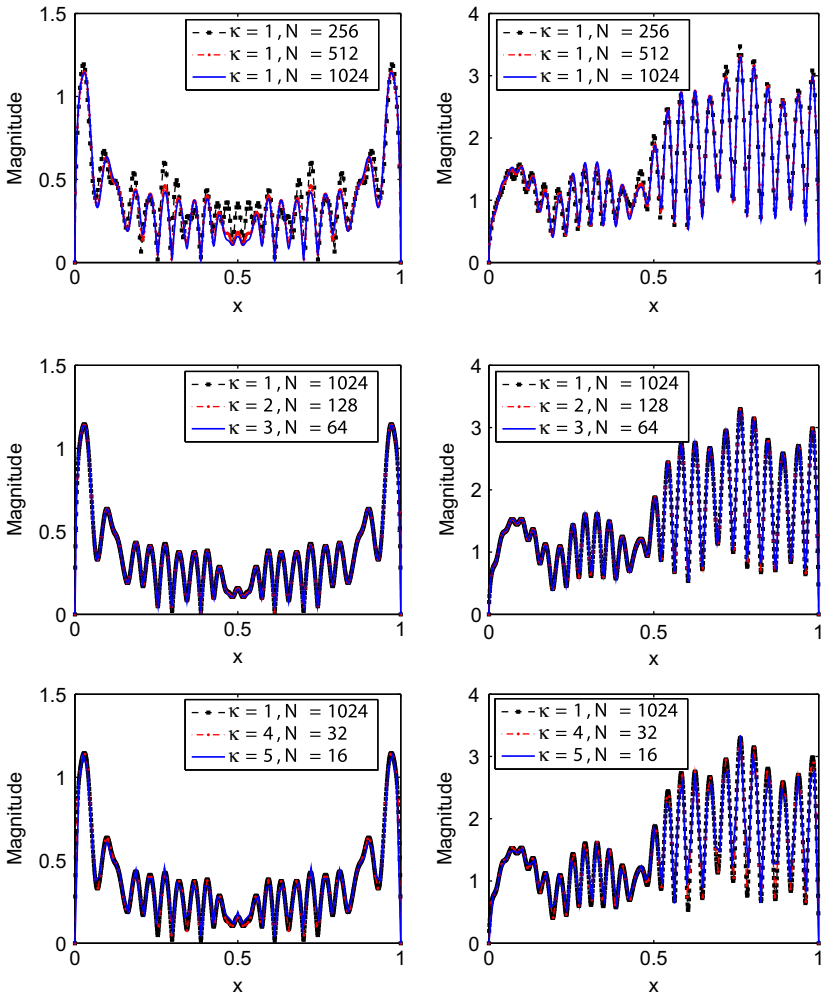


**Fig. 4.** Aperture electric field for Example 3 with $k_0 = 32\pi$ and $\varepsilon_r = 1$ computed by different approximations. Left: the angle of incidence $\theta = 0$. Right: the angle of incidence $\theta = \pi/4$.

$$\varepsilon_r(x,y)=\begin{cases}1, & 2/3\leqslant y<1,\\ 1.5, & 1/3\leqslant y<2/3,\\ 2, & 0\leqslant y<1/3.\end{cases} \tag{5.1}$$

*Example 3*

Consider a rectangular groove with 1 meter wide and 0.25 meter deep, i.e., $\Omega=(0,1)\times(0,0.25)$. The magnitude of the electric field (normal incidence) on the aperture of the cavity and the backscatter RCS for $k_0=2\pi$ and $\varepsilon_r=1$ or $4+\mathrm{i}$ are given in Fig. 3 compared with the experimental results in [26]. Numerical results are obtained by using our algorithm with $\kappa=1$ and $N=32$.

In Tables 4 and 5, we present the number of iterations of the preconditioned COCG solver for the interface system (4.4) with different wave numbers and different meshes. We observe that the number of iterations is independent of the number of unknowns and grows linearly with respect to the wave number $k_0$.

Finally, we compare the numerical results for Example 3 with the large wave number $k_0=32\pi$ and $\varepsilon_r=1$ computed by different approximations. In Fig. 4, we present the magnitudes of the fields on $\Gamma$ with the angle of incidence $\theta=0$ and $\theta=\pi/4$. It is obvious that high-order approximations require much fewer mesh points to fit the highly oscillatory field compared with low-order approximations. For example, at least 32 mesh points per wave length are needed when the low-order approximation $\kappa=1$ is used, while only 8 mesh points per wave length are needed when the high-order approximation $\kappa=4$ is used.

## 6. Concluding remarks

We have presented a tensor product Galerkin finite element method for electromagnetic scattering from a large cavity. A fast algorithm is also designed for solving the linear system arising from the cavity problem with layered media. Our algorithm may provide a preconditioner for two-dimensional problems with more general medium distribution. Numerical results illustrate the efficiency and accuracy of our method.

Numerical simulations for the cavity models have been done with various numerical methods. However, to the best of our knowledge, few theoretical analysis (stability analysis and error estimate) with the explicit wave number dependence has been obtained. Recently, stability estimates with explicit dependence on the large wave number and the depth of the cavity are given in [17,29,9]. However, they are not optimal. Based on the tensor product Galerkin finite element method proposed in this paper, numerical stability estimates with explicit dependence on the large wave number and the depth of the cavity can be obtained and will be reported elsewhere.

## Appendix A

In the appendix, we prove Theorem 3.3 by proving a more general case, i.e., the matrix $T=\left[t_{ij}\right]_{i,j=1}^{\kappa N-1}$ with

$$t_{ij}=\int_0^1\int_0^1 f(k_0|x-x'|)\left[k_0^2\psi_i(x)\psi_j(x')-\psi_i'(x)\psi_j'(x')\right]\mathrm{d}x\,\mathrm{d}x',\quad i,j=1,\ldots,\kappa N-1.$$

By the expression of $t_{ij}$ and the properties of the basis $\psi_i$, it is easy to prove that the matrix $T$ is bisymmetric.

In the following, for simplicity, let $\kappa_j^i$ denote the integer $\lfloor\frac{i}{\kappa}\rfloor-\left\lfloor\frac{j}{\kappa}\right\rfloor$ and let $i_\kappa$ and $j_\kappa$ be the integers satisfying $i=i_\kappa\mathrm{mod}\kappa$ and $j=j_\kappa\mathrm{mod}\kappa$, respectively. For $i,j=1,2,\ldots,\kappa N-1$, we have the following four cases.

Case (I): $i_\kappa=0$ and $j_\kappa=0$. Let

$$\begin{aligned}f^{(\mathrm{I})}(\kappa_j^i):=t_{ij}&=\int_{x_{[i/\kappa]-1}}^{x_{[i/\kappa]+1}}\int_{x_{[j/\kappa]-1}}^{x_{[j/\kappa]+1}} f(k_0|x-x'|)\left[k_0^2\psi_i(x)\psi_j(x')-\psi_i'(x)\psi_j'(x')\right]\mathrm{d}x\mathrm{d}x'\\ &=\int_0^1\int_0^1 f\left(k_0h\left|s-t+\kappa_j^i\right|\right)\left[k_0^2h^2L_\kappa(s)L_\kappa(t)-L_\kappa'(s)L_\kappa'(t)\right]\mathrm{d}s\mathrm{d}t\\ &\quad+\int_0^1\int_0^1 f\left(k_0h\left|s-t+\kappa_j^i-1\right|\right)\left[k_0^2h^2L_\kappa(s)L_0(t)-L_\kappa'(s)L_0'(t)\right]\mathrm{d}s\mathrm{d}t\\ &\quad+\int_0^1\int_0^1 f\left(k_0h\left|s-t+\kappa_j^i+1\right|\right)\left[k_0^2h^2L_0(s)L_\kappa(t)-L_0'(s)L_\kappa'(t)\right]\mathrm{d}s\mathrm{d}t\\ &\quad+\int_0^1\int_0^1 f\left(k_0h\left|s-t+\kappa_j^i\right|\right)\left[k_0^2h^2L_0(s)L_0(t)-L_0'(s)L_0'(t)\right]\mathrm{d}s\mathrm{d}t,\end{aligned}$$

where $\kappa_j^i \in \{2-N, 3-N, \ldots, 0, 1, \ldots, N-2\}$. Apparently, $f^{(\mathrm{I})}(\kappa_j^i) = f^{(\mathrm{I})}(-\kappa_j^i)$. Thus, there are at most $N-1$ different quantities in this case.

Case (II): $i_\kappa = 0$ and $j_\kappa \neq 0$. Let

$$\begin{aligned} f^{(\mathrm{II})}(j_\kappa, \kappa_j^i) := t_{ij} &= \int_{x_{\lfloor i/\kappa \rfloor - 1}}^{x_{\lfloor i/\kappa \rfloor + 1}} \int_{x_{\lfloor j/\kappa \rfloor}}^{x_{\lfloor j/\kappa \rfloor + 1}} f(k_0|x-x'|)\left[k_0^2 \psi_i(x)\psi_j(x') - \psi_i'(x)\psi_j'(x')\right] \mathrm{d}x\mathrm{d}x' \\ &= \int_0^1 \int_0^1 f\left(k_0 h\left|s - t + \kappa_j^i - 1\right|\right)\left[k_0^2 h^2 L_\kappa(s) L_{j_\kappa}(t) - L_\kappa'(s) L_{j_\kappa}'(t)\right] \mathrm{d}s\mathrm{d}t \\ &\quad + \int_0^1 \int_0^1 f\left(k_0 h\left|s - t + \kappa_j^i\right|\right)\left[k_0^2 h^2 L_0(s) L_{j_\kappa}(t) - L_0'(s) L_{j_\kappa}'(t)\right] \mathrm{d}s\mathrm{d}t, \end{aligned}$$

where $j_\kappa \in \{1, 2, \ldots, \kappa-1\}$ and $\kappa_j^i \in \{2-N, 3-N, \ldots, 0, 1, \ldots, N-1\}$. It follows from $L_\kappa(s) = L_0(1-s)$ and $L_{j_\kappa}(t) = L_{\kappa - j_\kappa}(1-t)$ that $f^{(\mathrm{II})}(j_\kappa, \kappa_j^i) = f^{(\mathrm{II})}(\kappa - j_\kappa, 1 - \kappa_j^i)$. Thus, the number of different quantities is at most $\frac{\kappa-1}{2}(2N-2)$ for odd $\kappa$ or $\left(\frac{\kappa}{2} - 1\right)(2N-2) + N - 1$ for even $\kappa$. Then, regardless of parity of $\kappa$, there are at most $(\kappa-1)(N-1)$ different quantities in this case.

Case (III): $i_\kappa \neq 0$ and $j_\kappa = 0$. Let

$$\begin{aligned} f^{(\mathrm{III})}(i_\kappa, \kappa_j^i) := t_{ij} &= \int_{x_{\lfloor i/\kappa \rfloor}}^{x_{\lfloor i/\kappa \rfloor + 1}} \int_{x_{\lfloor j/\kappa \rfloor - 1}}^{x_{\lfloor j/\kappa \rfloor + 1}} f(k_0|x-x'|)\left[k_0^2 \psi_i(x)\psi_j(x') - \psi_i'(x)\psi_j'(x')\right] \mathrm{d}x\mathrm{d}x' \\ &= \int_0^1 \int_0^1 f\left(k_0 h\left|s - t + \kappa_j^i + 1\right|\right)\left[k_0^2 h^2 L_{i_\kappa}(s) L_\kappa(t) - L_{i_\kappa}'(s) L_\kappa'(t)\right] \mathrm{d}s\mathrm{d}t \\ &\quad + \int_0^1 \int_0^1 f\left(k_0 h\left|s - t + \kappa_j^i\right|\right)\left[k_0^2 h^2 L_{i_\kappa}(s) L_0(t) - L_{i_\kappa}'(s) L_0'(t)\right] \mathrm{d}s\mathrm{d}t, \end{aligned}$$

where $i_\kappa \in \{1, 2, \ldots, \kappa-1\}$ and $\kappa_j^i \in \{1-N, 2-N, \ldots, 0, 1, \ldots, N-2\}$. Due to the symmetry with respect to Case (II), no any new quantity appears.

Case (IV): $i_\kappa \neq 0$ and $j_\kappa \neq 0$. Let

$$\begin{aligned} f^{(\mathrm{IV})}(i_\kappa, j_\kappa, \kappa_j^i) := t_{ij} &= \int_{x_{\lfloor i/\kappa \rfloor}}^{x_{\lfloor i/\kappa \rfloor + 1}} \int_{x_{\lfloor j/\kappa \rfloor}}^{x_{\lfloor j/\kappa \rfloor + 1}} f(k_0|x-x'|)\left[k_0^2 \psi_i(x)\psi_j(x') - \psi_i'(x)\psi_j'(x')\right] \mathrm{d}x\mathrm{d}x' \\ &= \int_0^1 \int_0^1 f\left(k_0 h\left|s - t + \kappa_j^i\right|\right)\left[k_0^2 h^2 L_{i_\kappa}(s) L_{j_\kappa}(t) - L_{i_\kappa}'(s) L_{j_\kappa}'(t)\right] \mathrm{d}s\mathrm{d}t, \end{aligned}$$

where $i_\kappa, j_\kappa \in \{1, 2, \ldots, \kappa-1\}$ and $\kappa_j^i \in \{1-N, 2-N, \ldots, 0, 1, \ldots, N-1\}$. It follows from $L_{i_\kappa}(s) = L_{\kappa - i_\kappa}(1-s)$ and $L_{j_\kappa}(t) = L_{\kappa - j_\kappa}(1-t)$ that

$$f^{(\mathrm{IV})}(i_\kappa, j_\kappa, \kappa_j^i) = f^{(\mathrm{IV})}(\kappa - j_\kappa, \kappa - i_\kappa, \kappa_j^i) = f^{(\mathrm{IV})}(\kappa - i_\kappa, \kappa - j_\kappa, -\kappa_j^i).$$

Thus, there are at most $\left(\frac{\kappa^2}{4} - \frac{1-(-1)^\kappa}{8}\right)(2N-1) - \left(\frac{\kappa}{2} - \frac{1-(-1)^\kappa}{4}\right)(N-1)$ different quantities in this case.

Totally, there are at most

$$(1+\kappa-1)(N-1) + \left(\frac{\kappa^2}{4} - \frac{1-(-1)^\kappa}{8}\right)(2N-1) - \left(\frac{\kappa}{2} - \frac{1-(-1)^\kappa}{4}\right)(N-1) = \frac{\kappa(\kappa+1)(N-1)}{2} + \frac{\kappa^2}{4} - \frac{1-(-1)^\kappa}{8}$$

different quantities in the matrix $T$.

Let $\mathrm{Toeplitz}(\alpha_{1-m}, \alpha_{2-m}, \ldots, \alpha_0, \ldots, \alpha_{n-1})$ denote the $m \times n$ Toeplitz matrix $[\alpha_{ij}]_{i=1,j=1}^{m,n}$ whose entries are specified by $\alpha_{ij} = \alpha_{j-i}$. Obviously, for $\kappa = 1, T$ is a symmetric Toeplitz matrix. For larger $\kappa$, let $\mathbf{p}$ be the permutation vector

$$[\kappa, 2\kappa, \ldots, (N-1)\kappa, \quad 1, \kappa+1, \ldots, (N-1)\kappa+1, \quad \ldots, \quad \kappa-1, 2\kappa-1, \ldots, \kappa N-1].$$

By the discussion above, we obtain the matrix $\widetilde{T} = T(\mathbf{p}, \mathbf{p})$ is a symmetric $\kappa \times \kappa$ block matrix with Toeplitz blocks. Here, we use MATLAB notations. In particular,

$$\widetilde{T} = \begin{bmatrix} T_{11} & T_{12} & \cdots & T_{1\kappa} \\ T_{21} & T_{22} & \cdots & T_{2\kappa} \\ \vdots & \vdots & \ddots & \vdots \\ T_{\kappa 1} & T_{\kappa 2} & \cdots & T_{\kappa\kappa} \end{bmatrix},$$

where $T_{11}$ is the $(N-1) \times (N-1)$ symmetric Toeplitz matrix

$$T_{11} = \mathrm{Toeplitz}\left(f^{(\mathrm{I})}(N-2), f^{(\mathrm{I})}(N-3), \ldots, f^{(\mathrm{I})}(2-N)\right),$$

for $i = 1, 2, \ldots, \kappa-1, T_{1,i+1}$ is the $(N-1) \times N$ Toeplitz matrix

$$T_{1,i+1} = \text{Toeplitz}\left(f^{(\text{II})}(i,N-1), f^{(\text{II})}(i,N-2), \ldots, f^{(\text{II})}(i,2-N)\right),$$

and for $i,j = 1,2,\ldots,\kappa-1$, $T_{i+1,j+1}$ is the $N \times N$ Toeplitz matrix

$$T_{i+1,j+1} = \text{Toeplitz}\left(f^{(\text{IV})}(i,j,N-1), f^{(\text{IV})}(i,j,N-2), \ldots, f^{(\text{IV})}(i,j,1-N)\right).$$

## References


[1] M. Abramowitz, I.A. Stegun (Eds.), Handbook of Mathematical Functions with Formulas, Graphs, and Mathematical Tables, Dover Publications Inc., New York, 1992. Reprint of the 1972 edition.
[2] A. Aimi, A. Carini, M. Diligenti, G. Monegato, Numerical integration schemes for evaluation of (hyper) singular integrals in 2D BEM, Comput. Mech. 22 (1998) 1–11.
[3] H. Ammari, G. Bao, A.W. Wood, Analysis of the electromagnetic scattering from a cavity, Jpn. J. Ind. Appl. Math. 19 (2002) 301–310.
[4] H.T. Anastassiu, A review of electromagnetic scattering analysis for inlets, cavities, and open ducts, IEEE Antennas Propag. Mag. 45 (2003) 27–40.
[5] I.M. Babuška, S.A. Sauter, Is the pollution effect of the FEM avoidable for the Helmholtz equation considering high wave numbers?, SIAM J Numer. Anal. 34 (1997) 2392–2423.
[6] G. Bao, J. Gao, P. Li, Analysis of direct and inverse cavity scattering problems, Numer. Math. Theory Methods Appl. 4 (2011) 335–358.
[7] G. Bao, J. Gao, J. Lin, W. Zhang, Mode matching for the electromagnetic scattering from three-dimensional large cavities, IEEE Trans. Antennas Propag. 60 (2012) 2004–2010.
[8] G. Bao, W. Sun, A fast algorithm for the electromagnetic scattering from a large cavity, SIAM J. Sci. Comput. 27 (2005) 553–574 (electronic).
[9] G. Bao, K. Yun, Z. Zhou, Stability of the scattering from a large electromagnetic cavity in two dimensions, SIAM J. Math. Anal. 44 (2012) 383–404.
[10] G. Bao, W. Zhang, An improved mode-matching method for large cavities, Antennas Wirel. Propag. Lett. IEEE 4 (2005) 393–396.
[11] A. Bayliss, C.I. Goldstein, E. Turkel, On accuracy conditions for the numerical computation of waves, J. Comput. Phys. 59 (1985) 396–404.
[12] S. Britt, S. Tsynkov, E. Turkel, A compact fourth order scheme for the Helmholtz equation in polar coordinates, J. Sci. Comput. 45 (2010) 26–47.
[13] S. Britt, S. Tsynkov, E. Turkel, Numerical simulation of time-harmonic waves in inhomogeneous media using compact high order schemes, Commun. Comput. Phys. 9 (2011) 520–541.
[14] O.P Bruno, F. Reitich, High-order methods for high-frequency scattering applications, in: Modeling and Computations in Electromagnetics, Lecture Notes in Computational Science and Engineering, vol. 59, Springer, Berlin, 2008, pp. 129–163.
[15] R.S. Callihan, A.W. Wood, A modified Helmholtz equation with impedance boundary conditions, Adv. Appl. Math. Mech. 4 (2012) 703–718.
[16] R.H. Chan, M.K. Ng, C.K. Wong, Sine transform based preconditioners for symmetric Toeplitz systems, Linear Algebra Appl. 232 (1996) 237–259.
[17] S.N. Chandler-Wilde, P. Monk, Existence, uniqueness, and variational methods for scattering by unbounded rough surfaces, SIAM J. Math. Anal. 37 (2005) 598–618.
[18] K. Du, A composite preconditioner for the electromagnetic scattering from a large cavity, J. Comput. Phys. 230 (2011) 8089–8108.
[19] K. Du, Two transparent boundary conditions for electromagnetic scattering from two-dimensional overfilled cavities, J. Comput. Phys. 230 (2011) 5822–5835.
[20] K. Du, A new preconditioner for the interface system arising in a fast Helmholtz solver, Comput. Math. Appl. 63 (2012) 794–806.
[21] K. Du, G. Fairweather, W. Sun, Matrix decomposition algorithms for arbitrary order $C^0$ tensor product finite element systems, submitted for publication.
[22] G. Fairweather, A. Karageorghis, J. Maack, Compact optimal quadratic spline collocation methods for the Helmholtz equation, J. Comput. Phys. 230 (2011) 2880–2895.
[23] X. Feng, Z. Li, Z. Qiao, High order compact finite difference schemes for the Helmholtz equation with discontinuous coefficients, J. Comput. Math. 29 (2011) 324–340.
[24] E. Howe, A. Wood, TE solutions of an integral equations method for electromagnetic scattering from a 2D cavity, IEEE Antennas Wirel. Propag. Lett. 2 (2003) 93–96.
[25] F. Ihlenburg, Finite Element Analysis of Acoustic Scattering, Applied Mathematical Sciences, vol. 132, Springer-Verlag, New York, 1998.
[26] J.M. Jin, The Finite Element Method in Electromagnetics, second ed., Wiley-Interscience [John Wiley & Sons], New York, 2002.
[27] R. Lee, T.T. Chia, Analysis of electromagnetic scattering from a cavity with a complex termination by means of a hybrid ray-FDTD method, IEEE Trans. Antennas Propag. 41 (1993) 1560–1569.
[28] C. Li, Z. Qiao, A fast preconditioned iterative algorithm for the electromagnetic scattering from a large cavity, Journal of Scientific Computing Online first 53 (2012) 435–450.
[29] H. Li, H. Ma, W. Sun, Legendre Spectral Galerkin method for electromagnetic scattering from large cavities, SIAM J. Numer. Anal. 51 (2013) 353–376.
[30] M. Medvinsky, S. Tsynkov, E. Turkel, The method of difference potentials for the Helmholtz equation using compact high order schemes, J. Sci. Comput. 53 (2012) 150–193.
[31] P.R. Rousseau, R.J. Burkholder, A hybrid approach for calculating the scattering from obstacles within large, open cavities, IEEE Trans. Antennas Propag. 43 (1995) 1068–1075.
[32] E. Turkel, D. Gordon, R. Gordon, S. Tsynkov, Compact 2D and 3D sixth order schemes for the Helmholtz equation with variable wave number, J. Comput. Phys. (2012), http://dx.doi.org/10.1016/j.jcp. 2012.08.016.
[33] T. Van, A.W. Wood, Finite element analysis of electromagnetic scattering from a cavity, IEEE Trans. Antennas Propag. 51 (2003) 130–137.
[34] H.A. van der Vorst, Iterative Krylov methods for large linear systems, Cambridge Monographs on Applied and Computational Mathematics, vol. 13, Cambridge University Press, Cambridge, 2003.
[35] H.A. van der Vorst, J.B.M. Melissen, A Petrov-Galerkin type method for solving $Ax = b$, where A is symmetric complex, IEEE Trans. Magn. 26 (1990) 706–708.
[36] Y. Wang, K. Du, W. Sun, A second-order method for the electromagnetic scattering from a large cavity, Numer. Math. Theory Methods Appl. 1 (2008) 357–382.
[37] Y. Wang, K. Du, W. Sun, Preconditioning iterative algorithm for the electromagnetic scattering from a large cavity, Numer. Linear Algebra Appl. 16 (2009) 345–363.
[38] A. Wood, Analysis of electromagnetic scattering from an overfilled cavity in the ground plane, J. Comput. Phys. 215 (2006) 630–641.
[39] W.D. Wood Jr., A.W. Wood, Development and numerical solution of integral equations for electromagnetic scattering from a trough in a ground plane, IEEE Trans. Antennas Propag. 47 (1999) 1318–1322.
[40] J. Wu, Y. Wang, W. Li, W. Sun, Toeplitz-type approximations to the Hadamard integral operator and their applications to electromagnetic cavity problems, Appl. Numer. Math. 58 (2008) 101–121.
[41] Z. Xiang, T.T. Chia, A hybrid BEM/WTM approach for analysis of the EM scattering from large open-ended cavities, IEEE Trans. Antennas Propag. 49 (2001) 165–173.
[42] M. Zhao, Z. Qiao, T. Tang, A fast high order method for electromagnetic scattering by large open cavities, J. Comput. Math. 29 (2011) 287–304.
[43] M. Zhao, Z. Qiao, T. Tang, A fast high order iterative solver for the electromagnetic scattering by open cavities filled with the inhomogeneous media, J. Comput. Phys., submitted for publication.